Biophysical Journal
Article

Biophysical Society

Nanosecond structural dynamics of intrinsically disordered β-casein micelles by neutron spectroscopy

Hiroshi Nakagawa,[1,2,3,*] Marie-Sousai Appavou,[2] Joachim Wuttke,[2] Michaela Zamponi,[2] Olaf Holderer,[2] Tobias E. Schrader,[2] Dieter Richter,[2] and Wolfgang Doster[4]

[1]Materials Sciences Research Center, Japan Atomic Energy Agency, Tokai, Ibaraki, Japan; [2]Forschungszentrum Jülich, Jülich Centre for Neutron Science at Heinz Maier-Leibnitz Zentrum, Garching, Germany; [3]J-PARC Center, Japan Atomic Energy Agency, Tokai, Ibaraki, Japan; and [4]Technische Universität München, Physik-Department, Garching, Germany

ABSTRACT β-casein undergoes a reversible endothermic self-association, forming protein micelles of limited size. In its functional state, a single β-casein monomer is unfolded, which creates a high structural flexibility, which is supposed to play a major role in preventing the precipitation of calcium phosphate particles. We characterize the structural flexibility in terms of nanosecond molecular motions, depending on the temperature by quasielastic neutron scattering. Our major questions are: Does the self-association reduce the chain flexibility? How does the dynamic spectrum of disordered caseins differ from a compactly globular protein? How does the dynamic spectrum of β-casein in solution differ from that of a protein in hydrated powder states? We report on two relaxation processes on a nanosecond and a sub-nanosecond timescale for β-casein in solution. Both processes are analyzed by Brownian oscillator model, by which the spring constant can be defined in the isotropic parabolic potential. The slower process, which is analyzed by neutron spin echo, seems a characteristic feature of the unfolded structure. It requires bulk solvent and is not seen in hydrated protein powders. The faster process, which is analyzed by neutron backscattering, has a smaller amplitude and requires hydration water, which is also observed with folded proteins in the hydrated state. The self-association had no significant influence on internal relaxation, and thus, a β-casein protein monomer flexibility is preserved in the micelle. We derive spring constants of the faster and slower motions of β-caseins in solution and compared them with those of some proteins in various states (folded or hydrated powder).

SIGNIFICANCE We characterize the structural dynamics of β-casein micelles in solution employing multiple methods, mainly quasielastic neutron scattering. Two relaxation processes are found on a nanosecond and a sub-nanosecond timescale in the β-casein micelles in solution. Interestingly, the self-association of β-casein (micellization) does not affect the internal structural dynamics. This is in contrast to folding/unfolding of a protein, in which the change of the atomic packing affects the internal structural dynamics. This study provides new insights about the effects of the structural and association states of proteins on their internal motions.

INTRODUCTION

That the specific and well-defined structure of proteins determine their biological function is one dogma of molecular biology. Less well established is the functional role of fluctuations about the average structure. A. Warshel, co-Nobel prize winner in 2013 for his computer simulations of protein function, argues "that flexibility interferes negatively with rate acceleration. Catalysis requires stereochemically rigid structures" (1). This conclusion certainly applies to the substrate-product transformation at the active site. However, ligand entry and exit require an opening of the well-shielded active site. Regulatory adjustments and protein folding need some degree of flexibility. Once a protein folds into a unique structure, the structural flexibility is relatively restricted because of the rational intrastructure interaction apart from the thermal fluctuations around the local minima in the free energy potential (2–4). In contrast, a natively disordered protein takes flexible and relatively

Submitted October 13, 2020, and accepted for publication October 13, 2021.

*Correspondence: nakagawa.hiroshi@jaea.go.jp

Editor: Jill Trewhella.

https://doi.org/10.1016/j.bpj.2021.10.032

extended conformations and plays an important role in the cell. Caseins are among the first proteins to be recognized as this class of protein and control the calcium phosphate sequestration (5).

Computer simulations of protein structures cover a pico- to nanosecond timescale. This overlaps with the range accessible to inelastic neutron scattering. In the late 1980s, MD simulations of small proteins were performed with little or no solvent (6–8). Experimentally, this situation was approximated by neutron scattering experiments performed with hydrated or dry protein powders. The major contribution of the experimental side, however, was the extension to subzero temperatures (9). Only at low temperatures and in the absence of bulk solvent, one can study the low frequency vibrations and density of the states of proteins (10). The preparation of hydrated powder samples was defined by infrared and calorimetric studies of the low temperature properties of protein hydration water (11). It could be shown that these samples are thermally stable below 0.4 g/g degree of hydration. At this hydration, molecular motions and often protein function is active in contrast to completely dehydrated samples. Hydrated samples are very useful for neutron scattering analysis; the low amount of solvent in powders not only reduces the background in the scattering data but also suppresses translational and rotational diffusion of a whole protein, which reduces the resolution of protein internal dynamics in solutions. Neutron scattering emphasizes the hydrogens, which constitute nearly half of the atoms in proteins. A particularly useful property of the proton is its large incoherent cross section, about 10 times larger than those of other atoms. As a result, 85% of the scattering amplitude of proteins is incoherent and reflects the hydrogen atoms (12). In contrast to simple synthetic polymers, a protein is a heterogenous single polypeptide chain consisting of 20 different amino acids. The dynamical information can be obtained as an averaged one. The contribution of the D_2O solvent at low hydration (<0.4 g/g) remains below 10% at wave vectors above $q \sim 0.5$ Å^{-1}. Protein solutions by contrast are dominated by the coherent scattering of the D_2O solvent. High protein concentrations (∼100 mg/mL) are often used for measurements to be able to differentiate with sufficient signal/noise ratio the incoherent protein from coherent solvent scattering (13). High protein concentrations often induce irreversible aggregation reactions if the molecules cannot be properly protected. In our measurements, we collected high quality spectra of β-casein at a concentration of around 80 mg/mL. It is noted that phosphorylation of caseins is an important posttranslational modification occurring after the synthesis of the polypeptide chain in the Golgi apparatus of the mammary epithelial cell under the action of protein kinases (14). β-casein is a highly amphiphilic calcium-sensitive phosphoprotein, displaying a pronounced self-association behavior. This milk protein is characterized by a highly polar, negatively charged N-terminal domain containing its five phosphoseryl groups and a highly nonpolar C-terminal domain. All the amino acid residues that are phosphorylated are located at the N-terminal. β-casein associates naturally with an increasing concentration and temperature (micellization), forming micelles of limited size in a fully reversible endothermic process (15–22). The critical micelle concentration for β-casein is below 1.5 mg/mL (23).

The possibility to study β-casein under reversible conditions in solution was an essential motivation to perform the neutron scattering investigation of the high concentrated protein solution. We have studied α-, β-, and κ-casein before in various states, dry, dehydrated, and in solution, together with other folded proteins by neutron time of flight spectroscopy (TOF) (13). The main question was as follows: How does protein structure affect their molecular motions, and how do they depend on the solvent? In previous low-temperature work with hydrated myoglobin, combining elastic and inelastic neutron TOF and neutron backscattering spectroscopy (NBS) (9), two processes could be identified: 1) non-Gaussian rotational transitions of side chains on a picosecond timescale, later assigned to methyl rotation (24), and 2) a Gaussian process, $\tau \sim 100$ ps, which could be assigned to water-dependent local residue diffusion (25). Recently, it could be shown that these two components account quantitatively for broadband and wide temperature range neutron scattering spectra of hydrated myoglobin (26,27). TOF spectroscopy in solution with various proteins could resolve only methyl rotation and global diffusion (13). The dynamic amplitude, but not the rate, varies with the protein structure. The disordered caseins exhibit larger dynamic amplitudes of rotational transitions than the compactly folded proteins. Moreover, anomalous global diffusion was significantly observed for α-, β-, and κ-casein; the diffusion rate $\Gamma \sim q^2$ extrapolates to a finite value at $q = 0$. This is an indication of an internal relaxation process for caseins, which is not clearly seen with folded proteins. The observation of this process with improved instrumental resolution motivated our neutron spin echo (NSE) and NBS experiments with β-casein in solution in this study. Another motivation was to examine if β-casein in solution and in powder state provide different quasielastic neutron scattering spectra in comparison of the literature by Perticaroli et al. (28) and Dhinsda et al. (29). We ask the question whether similar dynamic processes are observed or whether the bulk solvent induces additional molecular motions. The biological and industrial background of natively disordered β-casein has been excellently presented in the literatures (28,29) and is not discussed here again. Instead, we focus on neutron scattering experiments performed with other natively disordered proteins: the human τ-protein and its coupling to hydration water (30) and disordered myelin basic protein (MBP) studied in solution by NSE (31). Proteins with mostly disordered structures in their functional state are violating the basic dogma of molecular biology. In these cases, it is probably

the molecular flexibility and less the stereo-chemical rigidity that determines the biological function. The self-association of β-casein further allows us to study the interesting question of whether constraints within the micelle affect the molecular dynamics. The effect of association should be interesting to compare with folding/unfolding. A comprehensive review of "protein dynamics in solution" is presented by Grimaldo et al. (32).

MATERIALS AND METHODS

All neutron scattering experiments were performed using the Jülich Centre for Neutron Science (JCNS) instruments at the Maier-Leibnitz Zentrum (MLZ) in Garching, Germany. The curation of and access to raw data from large-scale research facilities is regulated by the facilities. For the instruments used in this work, MLZ ensures long-term preservation of all raw data. Our raw data are available upon request. The normalized and subtracted data of NSE and NBS are submitted as Supporting materials and methods.

Sample preparation

Bovine β-casein (C6905) was purchased from Sigma-Aldrich (St. Louis, MO). The number of amino acids is 209, and the molecular mass is 24 kDa. Its concentration was calculated based on the absorbance at 280 nm assuming an extinction of 4.6 (1%). The following sample conditions were used for all experiments: 0.1 M deuterated phosphate buffer (D_2O) pD = 6.9 with 1 mM EDTA and 0.1 M NaCl. The sample solutions were filtered using a 0.2-μm pore size just before the subsequent scattering measurements.

Dynamic light scattering

Dynamic light scattering (DLS) measurements were performed with the samples at a concentration of 82.6 mg/mL by employing an ALV 7004 digital correlator (ALV, Langen, Germany) at a laser wavelength of 514.5 nm. The scattering angles, θ, are 30, 90, and 150°, which correspond to the q-values of 0.0084, 0.023, and 0.031 nm^{-1}, respectively. The z-average diffusion coefficients and polydispersity indexes (PdI) were obtained from the cumulant expansion analysis. The detailed analytical descriptions in the analysis are shown in the section of S1. Polydispersity and Cumulant Analysis in DLS in Supporting materials and methods. The reversibility of the micelle association was tested by turbidity experiment in up and down temperature cycles, as shown in the section of S2. Thermal association and turbidity measurements in Supporting materials and methods.

Small-angle neutron scattering

Small-angle neutron scattering (SANS) measurements were performed using the KWS-1 instrument at the MLZ in Garching, Germany (33) at a neutron wavelength of λ = 7.0 Å and three different detector distances (4, 8, and 20 m). The accessible momentum transfers of $q = 4\pi/\lambda \sin(\theta/2)$, where θ is the scattering angle and λ is the wavelength, ranged from 0.022 to 1.0 nm^{-1}. Protein sample concentrations were 82.6 mg/mL, corresponding to volume fractions of 6.0%, respectively. The measurements were conducted at five different temperatures (10, 20, 40, 60, and 75°C).

A rescaled mean spherical approximation (RMSA) was applied to analyze the β-casein solution structure at elevated concentrations of 82.6 mg/mL. The intensity is described as $I(q) = P(q) \times S(q)$, where the sphere form factor is expressed by

$$P(q) = \left(3(sin(qR) - (qR)cos(qR))/(qR)^3\right)^2, \quad (1)$$

where R is the radius of the sphere. The radius of gyration is obtained by $R_g = \sqrt{3/5R}$. The expression for the RMSA structure factor was adopted from the literature (34,35). Data treatment and analysis were performed using the QtiKWS program (36). The SANS profiles are shown in Fig. S3.

NSE spectroscopy

The principles of NSE spectroscopy are decribed by Bee (37). NSE experiments were conducted using the J-NSE spectrometer at the MLZ in Garching, Germany (38) at four different neutron wavelengths (0.8, 1.0, 1.2, and 1.7 nm). The measurements were carried out at five different temperatures (5, 20, 40, 60, and 75°C) in the q-range of 0.4–1.9 nm^{-1}. The protein concentration was 84.3 mg/mL. A fresh sample solution was prepared for each temperature to avoid protein degradation because the counting time of the NSE spectrometer was relatively long (from several hours to an entire day).

NBS

Principles of NBS are explained by Bee (37). NBS measurements were performed at the instrument SPHERES at the MLZ in Garching, Germany (39). This instrument has an energy resolution (full-width at half maximum) of 0.67 μeV. Scattering wave vectors, q, range from 2.2 to 19 nm^{-1}, and the energy window is $\pm$30 μeV. Spectra at five different temperatures (5, 20, 40, 60, and 75°C) were collected for 8–10 h. The protein concentration was 81.7 mg/mL. The spectra of an empty cell and buffer at each temperature were subtracted from the solution spectrum, considering the volume fraction of a protein in solution. The buffer subtraction was performed by estimating the volume fraction from the typical specific volume, 0.74 mL/g (40). The detail is described in S4 of Supporting materials and methods. It is noted that in a recent publication, the buffer background subtraction was considered by including the water dynamics spectra for hydration water (41). This specific water background consideration procedure, although interesting, would deserve a particular examination for the applicability of this procedure to the natively unfolded protein of β-casein. It is, however, out of the here presented topic. As is will be shown later in this study, the coincidence of diffusion coefficients with the NSE supports the validity of the conventional subtraction method. A vanadium standard was used for normalization of the detectors and to define their spectral resolution functions. The spectral analysis was performed using the programs FRIDA (42), MathCAD14, and Origin61.

RESULTS

Spin echo spectroscopy (NSE): effect of temperature and wave-vector q

Fig. 1 displays the normalized intermediate scattering function, $I_c(q,t)$, of a β-casein micelle solution at various q-values at 5°C and 84.3 mg/mL. At this temperature, the fraction of β-casein monomers still plays a significant role (18). The measurements cover a time window of up to 40 ns and a q-range of 0.4–1.9 nm^{-1}, corresponding to a spatial scale of 3–16 nm. $I_c(q, t)$ exhibits a strong q-dependence with the correlation times decreasing with increasing q. The time decay follows a simple exponential law at lower q-range, exhibiting a strongly q-dependent correlation time according to $\tau_D = (q^2 \cdot D)^{-1}$, which is a characteristic feature of the

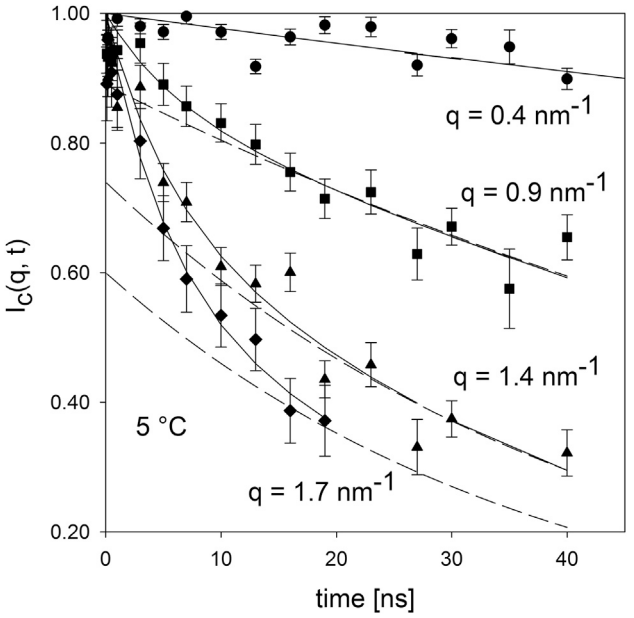

FIGURE 1 Normalized, coherent NSE intermediate scattering function, $I_c(q,t)$, of a β-casein micelle solution at 84.3 mg/mL and 5°C above the critical micelle concentration (CMC). The data are corrected for background and instrumental resolution. Full lines reflect two-component fits, comprising global diffusion and internal relaxation depending on q. The dashed lines show the contribution of global diffusion ignoring internal relaxation.

translational global diffusion with coefficient D. At higher q-range, the attempt to adjust the data to a single exponential component of micelle diffusion was not entirely successful. The systematic deviations from the monoexponential decay at a short time (below ~15 ns) emerges at q-values above 0.7 nm^{-1}, corresponding to a spatial scale of around 10 nm (approximately the size of the micelle (16,18)). This feature should thus indicate the presence of structural motions inside the micelles on a few nanoseconds timescale (43). Based on the above results, the intermediate scattering function, $I_c(q,t)$, can be modeled assuming a combination of global diffusion of whole micelles and structural motions. Accordingly, we can introduce a two-component model of the intermediate scattering function for NSE, as follows:

$$I_c(q,t) = I_1(q,t)exp\left(-q^2Dt\right), \tag{2}$$

$$I_1(q,t) = 1 - A_1(q) + A_1(q)exp(-t/\tau_1), \tag{3}$$

where $I_1(q,t)$ represents the intermediate scattering function of the structural motions, $A_1(q)$ is the amplitude of a second component of structural motions, and τ_1 is the correlation time. Fig. 2 shows the diffusion coefficient D at various temperatures and q-values. The diffusion speeds up with increasing temperature, but no significant q-dependence of D could be detected.

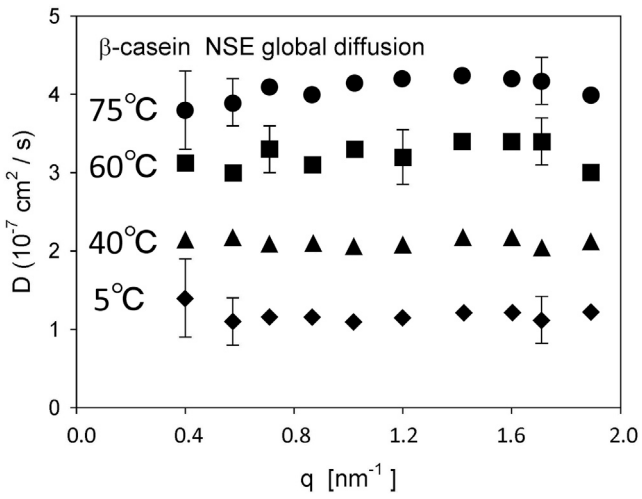

FIGURE 2 NSE diffusion coefficient of β-casein in solution, D(q,T) from fitting the NSE data illustrated by Fig. 1 to Eq. 2. The parameters of the internal process are displayed in Figs. 5 and 6. Error bars for all data are similar.

Micelle association and hydrodynamic radius

The diffusion coefficient does not properly reflect the state of association because the respective slowing down is compensated by the decreasing viscosity with increasing temperature. The Stokes radius corrects for the viscosity effect according to

$$R_H = k_BT/6\pi\eta D, \tag{4}$$

where η denotes the viscosity of the solvent. Fig. 3 shows the resulting hydrodynamic radius versus the temperature, reflecting the growth of micelle size. The figure combines

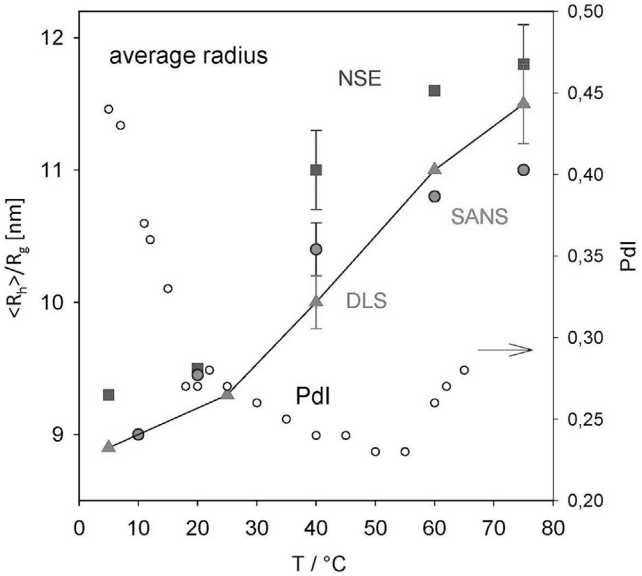

FIGURE 3 Radius of gyration R_g derived from SANS (*closed circles*), hydrodynamic radius R_H derived from DLS (*triangles*) and NSE (*squares*), and PdI derived from DLS (*open circles*).

results derived with SANS, NSE, and DLS from identical samples and conditions. In contrast to the random aggregation of globular proteins, β-caseins form reversible micelles of limited size (19). A limit of 11–12 nm in micelle size is reached at above 40°C. In the preassociation regime below 10°C, a consistent radius near 9 nm within error is deduced from the three above-mentioned methods. This coincidence is remarkable because different averages of the diffusion coefficients are involved: DLS, z-average; NSE, weight average; and SANS, mass average. Because the solution is transparent at 5°C, one could conclude that the respective size distribution has to be quite narrow. However, the DLS cumulant analysis yields a PdI, which is large at low temperatures and decreases to a plateau at high temperatures. The β-casein monomers have a reported Stokes radius of 3.7 nm and an extrapolated radius of gyration of 4.6 nm from gel permeation measurements and small-angle x-ray scattering measurements, respectively (44), confirming that in our system at 5°C, the molecules with R_H of 9 nm are strongly associated. For monodisperse solutions, the ratio R_g/R_H can serve as an index of structural compactness (45); for a rigid uniform sphere, the predicted ratio is 0.77, whereas for a flexible random coil in a good solvent, one expects 1.5. Accordingly, for β-casein, the observed ratio at low temperature is 0.95, suggesting that the predominantly monomeric chains adopt a somewhat extended conformation. At 75°C, the compactness index is still close to 0.95, whereas the heterogeneity index is diminished. It is noted that with the much larger β-casein micelles, the rates due to rotational diffusion are much slower than the translation widths and can be neglected in NSE and NBS, although in the case of small globular protein, the rotational diffusion needs to be taken into account. The detailed discussion is described in S5 in Supporting materials and methods.

Analysis of the NSE internal process: dynamic amplitude and relaxation time

We now focus on the initial short time component of $I_1(q,t)$ of NSE correlation function presented in Fig. 1. After correction for global diffusion, we analyze the initial phase up to ~15 ns in Fig. 1, according to Eqs. 2 and 3. Fig. 4 shows the $I_1(q,t)$, corrected for global diffusion, at two temperatures of 5 and 75°C and at q = 1.6 and 1.9 nm^{-1}. The decay of $I_1(q,t)$ is faster at higher temperature, indicating that the correlation time, τ_1, decreases with increasing temperature. In contrast, the limiting plateau value at long time varies only slightly with temperature, suggesting a larger mobile fraction at higher temperature. Compared with different $I_1(q,t)$ at different q, a lower plateau value at higher q was observed, indicating a larger mobile fraction. For more quantitative analysis, we fitted the initial short time component of $I_1(q,t)$ using Eq. 3, which is described by two parameters, $A_1(q)$ and τ_1. When keeping τ_1 fixed (q-global fits), q-dependent $A_1(q)$ was obtained, as shown

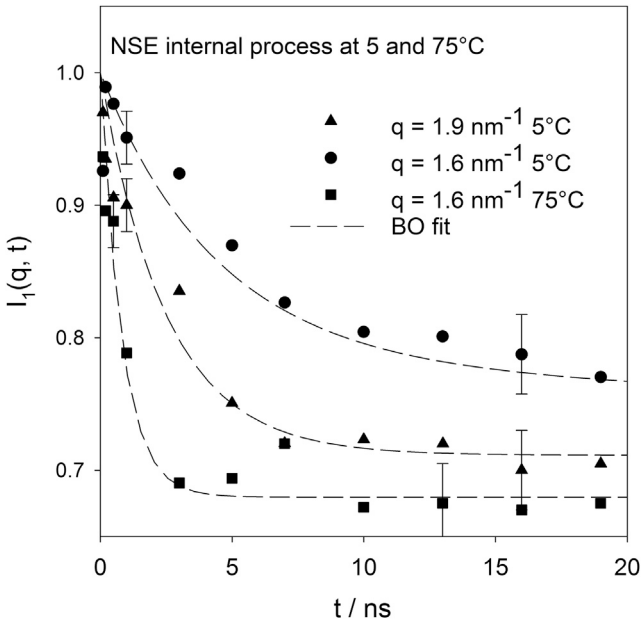

FIGURE 4 Intermediate scattering function $I_1(q,t)$ of the NSE structural relaxation process corrected for global diffusion at 5° (*triangles* and *circles*) and 75°C (*squares*) at two q- values 1.6 and 1.9 nm^{-1}. Exponential fits were performed with Eq. 7. The parameters are given in Figs. 5 and 6. The dashed lines represent the BO fitting curves.

in Fig. 5. In this case, q-independent relaxation time of τ_1 assumes that the structural motions are local process. The opposite case of keeping $A_1(q)$ fixed and varying τ_1 does

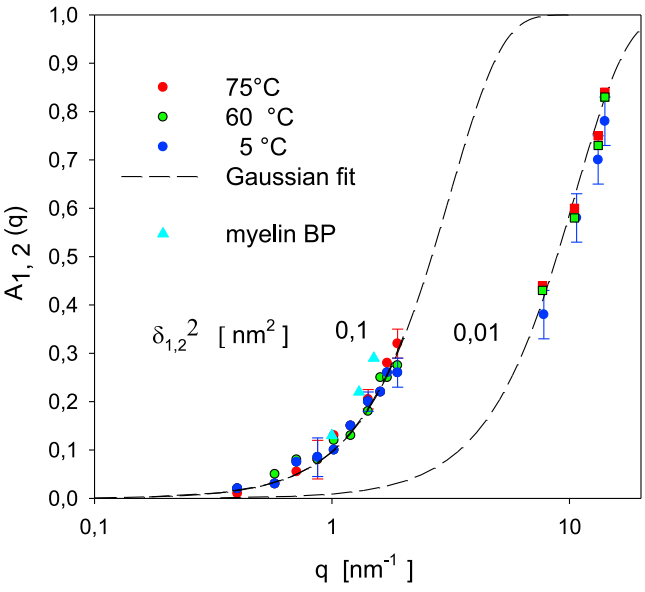

FIGURE 5 Quasielastic structure factors of NSE and NBS processes: $A_1(q)$, at three different temperatures based on fits NSE and NBS data by Eq. 3 and Eq. 5, respectively. Dashed lines represent fit assuming a Gaussian distribution of mean-square displacements, δ_1^2(NSE) = 0.1(±0.02) nm^2 and δ_2^2 (NBS, 5°C) = 0.01 (±0.005) nm^2. Circles and squares represent the NSE and NBS data, respectively. Light blue triangles represent disordered MBP (31). To see this figure in color, go online.

not account for the experimental data. A combined q-variation of both $A_1(q)$ and τ_1 cannot be completely excluded, but this case leads to uncertainties by parameter correlations when automatic fitting procedures are applied. Fig. 4 also shows the effect of temperature on $I_1(q,t)$ at fixed q; the relaxation time τ_1 decreases strongly when the temperature increases, whereas $A_1(q)$ is only slightly enhanced. Fig. 5 shows the quasielastic amplitude $A_1(q)$ of the NSE internal process versus q and temperature.

Fig. 6 shows an Arrhenius plot of the respective structural relaxation time τ_1 and the fit to the Arrhenius law: $\tau 1 = \tau_0 exp(H_1/RT)$. Protein internal dynamics should be characterized by activation energy, and in general, the relaxation time of a protein structure is dependent on temperature and viscosity (25). Accordingly, an Arrhenius plot should be reasonably defined. The resulting pre-exponential $\tau_0 = 0.3$ ps is in the microscopic range. The activation enthalpy of 22 kJ/mol is quite large, comparable to values observed with structural relaxation in aqueous solvents; dividing the relaxation time by the solvent viscosity removes most of the temperature dependence. The apparent activation enthalpy is reduced to less than 4 kJ/mol. This result indicates that the NSE structural relaxation process involves density fluctuations of the solvent.

NBS: effect of temperature and wave-vector q-dependence

Fig. 7 *A* shows the NBS spectrum of the β-casein solution at 5°C and two different q-values. The spectrum shown was obtained after the contributions of the sample cell and the D_2O buffer, properly adjusted for the missing protein volume, were subtracted. The strong q-dependence of the line width illustrates the dominant role of global diffusion. Global diffusion is the terminating slow process in the time domain. Therefore, diffusion broadening determines the effective resolution in the frequency domain with respect to slow internal processes. Apart from the narrow diffusion spectrum, a broader component indicates a second internal relaxation process, the "NBS structural relaxation process." Note that the spectra of the second component overlap on a logarithmic scale despite quite different q-values of 7.8 and 14.1 nm^{-1}. For translational diffusion, the respective linewidth would change by almost a factor of 3.22, considering $\sim q^2$. Because no such variation occurs in the broader component, we assign this component to a second local relaxation, which is different from NSE local relaxation.

For proteins in solutions, both localized internal motion and long-range global diffusion were considered to analyze the NBS data (13). The theoretical NBS spectrum $S_{inc}(q, E)$, which in this q-range is mainly incoherent (13), is as follows:

$$S_{inc}(q,E) = F(q)\cdot S_{res}(q,E) \otimes \left\{\frac{1}{\pi}\frac{q^2 D}{E^2 + q^2 D}\right\} \otimes \left[(1 - A_1(q))\delta(E) + \sum_{i=1\ or\ 2} \frac{A_i(q)}{\pi}\frac{\tau_i}{1 + E^2\tau_i^2} + B(q,E)\right], \quad (5)$$

where ⊗ represents the convolution operation in energy space, $S_{res}(q,E)$ is the resolution function (vanadium data), and B(q) is the background due to vibrational motions. F(q) is a scaling factor that includes the Debye-Waller factor. D denotes the casein micelle diffusion coefficient introduced in connection with the NSE experiments, except that the q-range is much larger, between 2 and 14 nm^{-1}. In Eq. 5, the two- and three-components fitting function include single and double Lorentzian, respectively. Because the NBS samples were identically prepared as for the NSE samples, we assume a common diffusion coefficient as a first step to constrain the fitting procedure. To test the stability of this assumption, in a second step, the D(q) parameter is allowed to float. In all cases, the required adjustments were within the error of the analysis. Therefore, we could not detect a significant variation of D(q) by the two neutron scattering techniques. It should be emphasized that the employed protein concentration of 81.7 mg/mL is rather moderate for the NBS technique. Thus, the quality of the NBS analysis profits from the additional requirement of consistency with the results derived before with NSE. For demonstration, we focus on two low-noise detectors at q = 8 and 14 nm^{-1}, in which the data could be evaluated on a logarithmic scale. Fig. 7 *B* shows that the diffusion broadening at 5°C and 7.8 nm^{-1} is only slightly above the width of

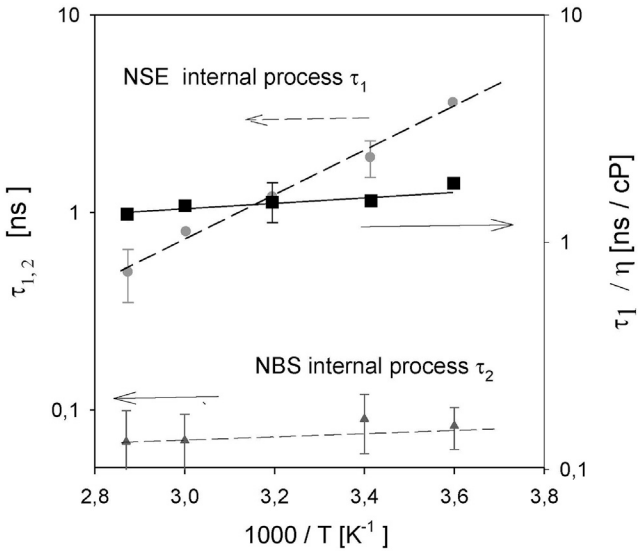

FIGURE 6 Arrhenius plots. Circles represent NSE internal relaxation time $\tau_1(T)$, dashed line represents fit to Arrhenius law, pre-exponential represents $\tau_0 = 0.3$ (±0.03) ps, and activation enthalpy represents $H_1 = 21.8$ (±0.5) kJ/mol. Squares represent relaxation time divided by the solvent viscosity, τ_1/η. The full line is the Arrhenius fit, and the activation enthalpy is now reduced to 4 (±1.5) kJ/mol. Triangles represent NBS internal relaxation time $\tau_2(T)$, according to Eq. 8.

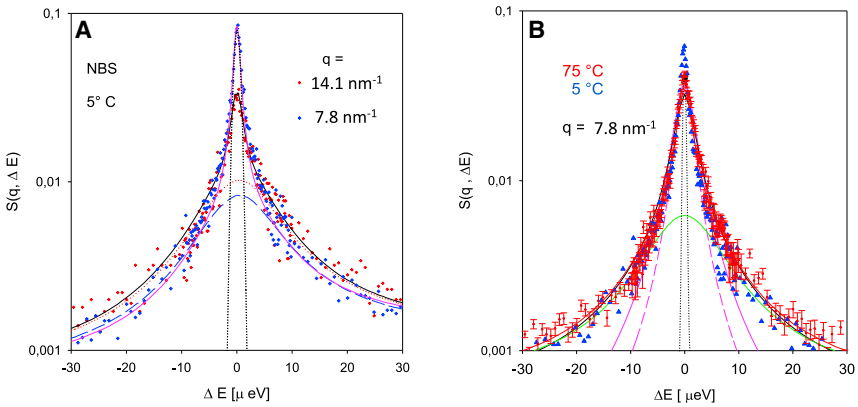

FIGURE 7 Backscattering spectrum of β-casein in solution at 81.7 mg/mL. (*A*) Shown is the backscattering spectrum (a.u.) on a logarithmic scale log[S(q, $\Delta E = \hbar\omega$)]at q = 7.8 (*blue*) and 14.1 (*red*) nm^{-1} and 5°C. Pink dashed line represents two-component fit (diffusion and internal relaxation) at q = 7.8 nm^{-1}; black line represents two-component fit at q = 14.1 nm^{-1}; broad dashed and dotted lines represent NBS internal relaxation at 7.8 and 14.1 nm^{-1}, respectively; and dotted black line represents instrumental resolution. Error bars are comparable to those in Fig. 7 *B*. (*B*) Backscattering spectra of a β-casein solution (a.u.) at q = 7.8 nm^{-1} and 5°C (*blue triangles*) and at 75°C (*red dots*). Dotted black line represents resolution function, pink dashed line represents diffusion broadening at 75°C, pink line represents diffusion broadening and NSE internal relaxation at 75°C, and green line represents NBS internal relaxation at 5°C. The asymmetric spectra in (*A*) were corrected during the analysis process. Error bars are shown at 75°C, and those of 5°C are comparable to those at 5°C. To see this figure in color, go online.

the instrumental resolution. To fix D(7.8 nm^{-1}, 5°C) = 1.2×10^{-7} cm^2/s requires a consistency check with the NSE experiment at the same temperature at lower q in Fig. 1. Apart from the narrow line due to global diffusion, a broader less q-dependent spectrum (Fig. 7 *A*) emerges at both q-values. The fit to Eq. 5 yields a quasielastic fraction $A_2(q)$ of 0.6 ($\pm$0.02) at q = 10.1 nm^{-1}, about twice the value observed for the NSE process at the maximal q = 1.9 nm^{-1} in Fig. 5. The quasielastic amplitude is reduced at the lower q-value of 7.8 nm^{-1}. This is shown in Fig. 5, together with a fit assuming a Gaussian displacement distribution, in which fitting function is the same as Eq. 5. The resulting δ_2^2 ~0.01 nm^2 is about 10 times smaller than δ_1^2. The NBS relaxation thus involves much smaller displacements than the NSE process. An internal correlation time τ_2 ~100 ps is derived as shown in Fig. 6. This is to be compared with $\tau_1 \approx 600$ ps for the NSE process at 5°C. Fig. 7 *B* displays two spectra at fixed q but very different temperatures, 5 and 75°C, on a log scale. Two- and three-component fits were performed. The NBS internal process (*green line*, Fig. 7 *B*) varies marginally between the two temperatures. At 75°C, it was possible, applying a three-component fit, to demonstrate that the additional broadening of the NBS diffusion line by the slow NSE relaxation process. This demonstrates the consistency of the dynamic models.

DISCUSSION

Subdiffusion of protein domains: the Brownian oscillator model

According to Fig. 6, the NSE internal relaxation time, τ_1, varies with the temperature proportional to the solvent viscosity. In general, such a simple relation was established for the visco-elastic relaxation of liquids by Maxwell in 1867 (46):

$$\tau = \eta / G_\infty, \qquad (6)$$

where η denotes the long timescale relaxed Newtonian viscosity, and G_∞ is the short timescale unrelaxed elastic shear modulus. Equation 6 applies not only to liquids but accounts also for the rates of ligand entry and exit reactions of a compact protein (47,48). The viscosity was adjusted using various glass-forming solvent mixtures, like 75% glycerol/water. At viscosities near 100 cP, the respective modulus yields $G_\infty \sim 10^{11}$ cPs^{-1} (0.1 GPa) at a Maxwell relaxation time of $\tau \approx 1$ ns. If stress is applied on a shorter time scale, the response is elastic, as the liquid behaves as a glass. In low-temperature studies of microscopic protein dynamics, the α-relaxation of hydration water plays an important role (9,11). The NSE process of β-casein in aqueous solution, at solvent viscosities of 1 cP and $\tau_1 \approx 1$ ns, yields $G_\infty \sim 10^9$ cP/s (0.001 GPa), about a factor of 100 less than for viscous solvents. G_∞ is closely related to the Young's modulus E by 1/3 E < G_∞ < 1/2 E. For dry β-casein powder, a Young's modulus of 7 GPa was determined and 9.7 GPa for the compact β-barrel protein GFP (28). The characteristic density relaxation rate will thus depend on the scale, increasing with q according to $\Gamma_D(q) = Dq^2$. Above $q = q_{max} \sim 1/d$, on the scale of the intermolecular distance (d), the diffusion rate levels off at the α-relaxation rate $\Gamma_D(q > 2\pi/d) \sim \tau^{-1}$. The liquid structural relaxation becomes q-independent and thus localized at high q. With protein structural relaxation, one expects localized dynamics and thus q-independent correlation times at all q. The most popular model among neutron scatterers, analyzing protein residue motions, is the "diffusion inside a sphere" model (49). This model predicts an effective line width, which increases with q above q_S with $q_S = 2\pi/r_S$, r_S being the radius of the sphere. Although the crossover at q_S was never really observed, q-dependent effective rates were often explained by free diffusion with rigid boundaries. From the elastic incoherent structure factor of α-amylase, the radius of the spheres, r_S = 1.2 Å (native) and 1.8 Å (unfolded), was obtained, which leaves little space to free diffusion (50). In his more recent work, Volino (49) votes

for a continuous phenomenological "Gaussian model" with soft boundaries. He introduces a joint Gaussian probability distribution of a particle, assuming different positions at two different times. Because the positions are not independent, the distribution is "joint" by a two-time correlation coefficient. This joint probability distribution has been derived before as the solution of the Smoluchovski equation of a harmonically bound particle (51). It is known as the Ornstein-Uhlenbeck process in the overdamped case. The parabolic potential of a harmonic oscillator and its Gaussian displacement distribution seems a plausible approximation to continuous residue motions. The latter was analyzed recently by the Brownian oscillator (BO) model (52). The BO model is also discussed in Grimaldo et al. (32). The BO leads to a remarkably compact time domain intermediate scattering function, which can be easily applied to evaluate experimental data. The powder averaged three-dimensional BO correlation function reads (52,53):

$$I_{BO}(q,t) = exp\{ -q^2\delta^2[1 - exp(-t/\tau_{BO})]\}, \qquad (7)$$

$\delta^2 = <u_x^2>$ denotes the x-component of variance of the isotropic three-dimensional displacement.

$$\delta^2 = k_BT/(m\omega_0^2) = k_BT/K, \qquad (8)$$

where K is spring constant of the isotropic parabolic potential: $F = K\cdot u_r^2$ with $<u_r^2>/3 = <u_x^2> = <u_y^2> = <u_z^2>$. The BO relaxation time is given by $\tau_{BO} = \delta^2/D_L$, where D_L denotes the effective local diffusion coefficient. At short times, $t << \tau_{BO}$, the particle performs long-range diffusion, $<\tau_{BO}>^{-1} = D_L\cdot q^2$. At long times, the BO intermediate scattering function tends to a constant, the elastic fraction named $EISF(q) = 1–A_1(q)$, and $A_1(q)$, denotes the "quasielastic fraction" or the dynamic amplitude:

$$I_{BO}(q, t \gg \tau_{BO}) = 1 - A_1 = exp(-q^2\delta^2) \qquad (9)$$

Equation 7 deviates only slightly from an exponential function; the fits to the data in Fig. 1 thus yield within experimental error the same parameters as those shown in Figs. 5 and 6. Accordingly, the q-dependence of $A_1(q)$ is rather well explained by a Gaussian distribution of displacements; the variance is $\delta_1^2 \approx 0.1$ nm^2. This is much larger than the diffusive displacements observed in folded proteins, such as $\delta^2 \sim 0.1$ Å^2 in hydrated myoglobin (27). Because the relaxation time varies with the solvent viscosity, $\tau_1 \sim \eta$, as for global diffusion, it appears that the NSE process reflects subglobal diffusion of entire protein domains.

Stadler et al. (31) investigated "intrinsically disordered" MBP, applying the same NSE method and covering the same time and q-range. These authors also observe a fast component (initial decay) in the intermediate scattering function. Their Fig. 3 *A* strikingly resembles the β-casein data of Fig. 1. The β-casein data show a more pronounced fast component, possibly because the protein concentration was ~50% larger. Moreover, the correlation time τ_1^{MBP} ~8.4 ns overlaps with the results of Fig. 6. Fig. 5 shows that even the dynamic amplitudes $A_1(q)$ in these unfolded proteins are nearly identical. Thus, one can assume a similar nature of these processes despite different amino acid sequences. Stadler et al. (31) apply the Zimm model of random polymer chains to MBP, which is a coarse-grained description of flexible beads: N beads of fixed length are connected by entropic springs. It predicts a number of relaxation modes; the slowest mode is overall rotation (31). It neglects internal friction or motions that occur at length scales shorter than the beads, such as hindered dihedral rotations, side-chain interactions, and hydrogen bonding. This is the range of the NBS internal processes at the timescale τ_2. The Zimm model and even more sophisticated extensions do not explain the NSE data of MBP. One has to take into account that MBP is not fully unfolded but retains a compact core and a folded secondary structure content of 44%. Thus, one expects slower dynamics than for the ideal random polymer chain. This conclusion is supported by the index of compactness, the ratio of R_g/R_h, which is close to 0.91. A Gaussian chain would yield 1.5. For a compact native protein like myoglobin, one obtains 0.79, close to the limit of a rigid sphere of $(3/5)^{1/2} = 0.775$. Fig. 3 shows that this ratio evolves for β-casein from 1.3 at low temperatures, mostly monomers, to 0.91 at high temperatures, after the formation of micelles is established.

Protein spring constants in folded and unfolded states

Bicout and Zaccai (54) proposed in 2001 to determine protein spring constants (K) from the temperature slopes of the mean-squared displacements with hydrated protein powders. It was even proposed to explain the enhancement of displacements at "the dynamical transition" by a softening of the protein spring constants. Above the transition, K ~0.3 N/m was obtained for hydrated myoglobin (54). The effective vibrational spring constant of hydrated myoglobin was 10 N/m (9). A high temperature spring constant of hydrated myoglobin was recently derived by fitting backscattering data to the BO model in the time domain: $\delta_2^2 = 0.11$ Å^2 and K = 3.8 N/m (27), much larger than the Zaccai results (54). Hydrated β-casein with a time constant around 100 ps yields K = 0.4 N/m (28), whereas for the similar NBS process in solution, a nearly identical spring constant is derived: K = 0.38 N/m. The slow NSE process ($\delta_1^2 = 0.1$ nm^2) is characterized by a spring constant K (1 ns) = 0.04 N/m at 300 K (Eq. 8), 10 times less than K at 100 ps obtained by NBS. Interestingly, spring constant K at 100 ps is independent of sample conditions, powder, and solution. Stadler et al. derive the internal dynamics of MBP from the fast initial phase at 8 ns displacements, which is similar to those of β-casein (31). The resulting spring constant of MBP in solution is K (300 K, 10 ns) = 0.08 N/m. This result was

interpreted as the coupling of different protein domains. The spring constant is about a factor of two larger than K of β-casein at the same conditions. The spring constants as determined from the diffusion method for Taq polymerase and ADH are 10 times smaller and overlap with the range measured with atomic force microscopy (AFM) (43,55,56). The AFM method, however, probes the protein elasticity on a much longer timescale (ms) than neutron scattering (ns) (55). The small spring constants derived with neutron scattering are thus surprising. The method by Bicout and Zaccai (54) involves the crossover region of relaxation time and instrumental resolution time, which may explain some differences. Most striking are the nearly identical force constants determined for the NBS relaxation of β-casein, hydrated and in solution, suggesting that the relevant structural process should be decoupled from the bulk solvent. Moreover, nearly identical values were observed for the NSE process of two unfolded proteins in solution: β-casein and MBP. These spring constants discussed above are summarized in Table 1.

Comparison of internal rate coefficients of hydrated folded proteins and β-casein in solution

In a comprehensive study, Gaspar et al. (13) compare the dynamics of three globular proteins and three unfolded caseins in different states, dry, hydrated, and in solution, using neutron TOF. Two distinct spectral components were identified; the broad component displayed a q-independent line width, corresponding to a 5-ps timescale, which was assigned to methyl rotational transitions. The linewidth of the second narrow component varied with q^2 and was thus assigned to translational diffusion. Fig. 8 shows the methyl transition rates in myoglobin (hydrated and in solution) and for β-casein in solution. Also, the rates of the alanine-dipeptide methyl side chain are displayed (25). This shows that the torsional rate coefficients are rather independent of structure, degree of hydration,

TABLE 1 Spring constants K determined with different instruments and methods

Protein	State	Process	δ^2/Å^2	τ/ps	K [N/m]	Reference
myoglobin	hydrated	vibration	0.04	1	10	(9)
myoglobin	hydrated	NBS/BZ	0.04	100	0.3	(54)
myoglobin	hydrated	NBS/BO	0.11	100	3.8	(27)
MBP (F)	hydrated	NBS/BZ	1	100	0.185	(30)
Tau (UF)	hydrated	NBS/BZ	1	100	0.096	(30)
β-casein	hydrated	NBS/BO	1	100	0.4	(28)
β-casein	solution	NBS/BO	1	100	0.4	present
β-casein	solution	NSE/BO	10	1000	0.04	present
Myelin (UF)	solution	NSE/BO	5	8000	0.085	(31)
ADH (F)	solution	NSE/Diff	70	75,000	5.5×10^{-3}	(43)
Taq (F)	solution	NSE/Diff	50	50,000	8×10^{-3}	(56)
P-sel (F)	solution	AFM	81	ms	4×10^{-3}	(55)

BO, displacements δ^2 and respective resolution time, τ; BZ, Bicout/Zaccai (54); F, folded; NSE/Diff, determined with the diffusion/structure method (43,56); UF, unfolded.

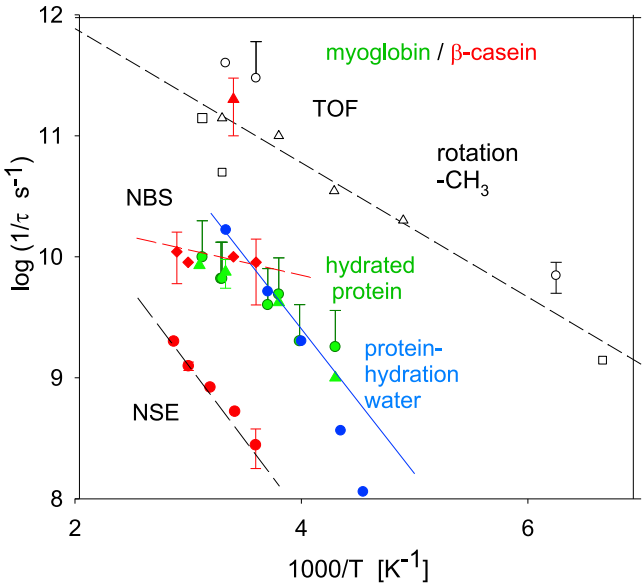

FIGURE 8 Arrhenius plot of protein internal relaxation rates. Red circles and diamonds represent β-casein solution, green triangles and circles represent hydrated myoglobin, blue circles represent hydration water of perdeuterated phycocyanin (24), red triangle represents methyl torsional rate of β-casein, open triangles represent methyl torsional transition rates myoglobin, and squares represent alanine dipeptide (24). To see this figure in color, go online.

or wave-vector q. With dehydrated and vitrified proteins, methyl rotations are the only molecular process observed with neutron scattering (24). With D_2O-hydrated myoglobin (9), a second dynamic component, displaying a Gaussian displacement distribution, was identified with NBS. In Fig. 8, the respective rate coefficients are displayed for hydrated myoglobin as green dots. This process overlaps with the α-relaxation of protein hydration water with H_2O-hydrated sample (blue dots), which gives rise to a "protein dynamical transition." It was thus assigned to water-coupled local residue diffusion. The respective squared displacement $\delta_2^2 \approx 1$ Å^2 (0.01 nm^2) is, however, significantly larger than the analogous values found with compact proteins (0.11 Å^2). The respective squared displacement $\delta_2^2 \approx 1$ Å^2 (0.01 nm^2) is significantly larger than the analogous values found with compact proteins (0.11 Å^2). The temperature dependence of local residue diffusion for both cases is much weaker than for the viscosity. This process is thus decoupled from the bulk solvent, as is also observed in the spring constant analysis (see former section), but depends crucially on the degree of hydration water. The NBS relaxation process of β-casein is Gaussian, which is well represented by a BO model (Fig. 5).

It was found that the q-dependent diffusion rate does not extrapolate to zero at q = 0 (13), as follows:

$$\Gamma_{TOF} = q^2 D + \Gamma_{int} \tag{10}$$

The offset, Γ_{int}, suggests the q-independent internal process with sub-nanosecond timescale. Although quantitative

analysis of the internal process was not possible because of the limited energy resolution of TOF, this offset was not clearly observed in the folded protein, and thus, the presence of casein-specific dynamics was predicted to be observed by neutron spectrometers with a higher energy resolution, NSE, and NBS. Although the TOF resolution of 30 μeV is not sufficient to detect the NBS fast local process on ∼100 ps directly, this process would give rise to a line width of 5 μeV in NBS spectra, which is consistent with the offset in the TOF. In the pioneer study, Perez et al. (57) compared the TOF spectra of myoglobin and lysozyme in their dry and hydrated state with a 60 mg/mL protein solution. After correcting for the solvent and translational and rotational diffusion of the protein, they could characterize an internal process on 5–8 ps depending on the sample preparation, solution, or hydrated powder. According to the quasielastic structure factors, solvated proteins in solution were more flexible than hydrated or dehydrated systems, and lysozyme was more flexible than myoglobin. It was probably the first assignment of this torsional motion to methyl rotation (9). Gaspar et al. (13) compared the same globular proteins. Therefore, it should be reasonable to consider that they have both the same origins. The TOF spectra also show an additional broad component of the relaxation faster than the slow (NSE) and the fast (NBS) internal motions, regardless of the conformational states (13). The third process is referred to as "ultrafast" internal motion. The respective line width of 150 μeV corresponds to a relaxation time of 4.4 (±0.2) ps. This process is too fast to be detected by NSE and NBS. A process occurring on a similar timescale was assigned to torsional transitions of mainly methyl groups in several globular proteins (27), which was characterized by non-Gaussian process (27). A similar NBS relaxation process was reported for the molten globule states of myoglobin (200 ps), ADH (160 ps), hemoglobin in blood cells (120 ps), and bacteriorhodopsin (120 ps) (58).

In principle, the self- and pair correlation functions for the same system are distinct. This was demonstrated in the case of the disordered polymer chain dynamics with the Zimm and Rouse models (59). Then, in the case of a protein, it is reasonable to think that the respective time dependence of the residue displacements is different as well. However, they share a common feature: the average relaxation times of the respective correlation functions are similar. In this case, this indicates that NSE and NBS record the same structural relaxation process with coherent and incoherent scattering, most likely exhibiting similar average relaxation times despite differing scattering functions. As for a diffusion coefficient, the same diffusion coefficients within error are obtained with both methods of NSE and NBS, which were measured above the structural factor peak. The detailed descriptions are shown in the section of S6. Diffusion coefficients and structure factor of the β-casein micelle in solution in Supporting materials and methods.

Perticaroli et al. (28) investigated β-casein in its hydrated states with and without calcium using TOF and NBS. The authors observe two spectral components, which were assigned to methyl rotation and NBS local structural diffusion. The latter has very similar features like the NBS process observed in solution. In addition, we observe in solution the NSE structural relaxation process on a nanosecond timescale. Its dependence on the bulk viscosity shows that it requires the existence of the bulk solvent. The former methyl rotation corresponds to non-Gaussian process, as discussed in the former section in β-casein in solution. Interestingly, this process seems to be independent of sample conditions, powder, or solution. Dhinsda et al. (29) studied β-casein in its hydrated and dehydrated states with NBS within a large temperature range. They observe in the temperature-dependent displacements two dynamical transitions resembling the original data published with hydrated myoglobin (9,27). They were assigned also to methyl rotation and hydration water-coupled local structural diffusion. Dhinsda et al. (29) Fourier transform the spectral data and derive a relaxation time near 12 ps, which is close to methyl rotation but far from the NBS-coupled relaxation process in solution with the timescale of ∼100 ps. The elastic incoherent structure factor (EISF) in the hydrated state also resembles the methyl rotation structure factor. The elastic fraction levels off at ∼0.7, which is assigned to immobilized protons. There is no Gaussian process observed. These results contrast with those of Perticaroli et al. (28), in which a 100-ps process is found in hydrated β-casein, which is consistent with our solution data.

Structural and dynamic heterogeneity of concentrated β-casein solutions

β-casein undergoes an endothermic self-association, resulting in a distribution of micelles of variable size. Apart from the increase of the average radius with temperature, the width decreases, as indicated by the drastic decrease of the PdI in Fig. 3. Similar deviations from monodispersity in the diffusion coefficients are not observed with NSE, most likely because the available time window is not wide enough to define a second cumulant in addition to a first cumulant. All spectra could be fitted assuming a "homogeneous" superposition of four "distinct exponential" processes. This applies even to the slightly nonexponential BO; the derived parameters are thus not obviously distributed. One could argue that the dynamic complexity is hidden by too large error bars. This possibility cannot be excluded, but this argument would apply to the majority of related experiments. It is also possible that for disordered proteins in solution, the dynamic heterogeneity is averaged out by "motional narrowing." We have recently studied the question of dynamic heterogeneity with dry and hydrated proteins (27).

Functional aspects

β-casein is just one component forming the casein micelle together with α- and κ-casein chains. Functional studies have to include the calcium phosphate binding capabilities. We have studied previously the size distribution of pressure-decomposed casein micelles by DLS and AFM, including the role of Ca phosphate particles (21,60). In this work, various structural models of casein micelles and the thermodynamics of association-dissociation are discussed. The main goal of these experiments was to determine the various interactions, which stabilize the casein micelle under conditions close to native milk. This was done by using the destabilizing action of pressure by determining the critical pressure of the stability limit for the associated micelle. We observe that the stability decreases with increasing size of the heterogeneous distribution, and it increases with increasing temperature, pH, and calcium concentration. The pressure-induced transition was biphasic, suggesting two well-defined micelle states M1 and M2 with different properties. Our experiments indicate that M2 is the β-casein-rich state, whereas M1 is mostly composed of α-casein forming the framework of the micelle. The relative population varies with external conditions in a reversible manner. M2 is less populated than M1 at ambient temperature because of its higher enthalpy but becomes more populated at higher temperatures because of a higher entropy. M2 is more stable than M1 at high pH and Ca concentration. We conclude that β-casein can dissociate reversibly from the micelle M2 without causing complete disintegration. The infrared spectra in the single band between phosphorus and oxygen (P-O) stretching region show that Ca_2P is already 30% dissociated from the micelle at 100 MPa. This suggests a coupled equilibrium between β-casein and Ca_2P binding to the micelle. In the presence of calcium, the dissociation becomes irreversible because of the formation of calcium phosphate particles. To achieve these results, it was essential to perform in situ static and dynamic light backscattering experiments at high pressures with turbid solutions at casein concentrations comparable with those of native milk. The variation in size of intact micelles follows a log-normal distribution at ambient and elevated pressures, like Fig. 9 in this study, suggesting a Gaussian distribution of stabilization-free energies. Caseins form heterogeneous micelles, stabilized by a variety of interactions. Their understanding can facilitate the control of the aggregation of casein, which is an important aspect of milk product fabrication. In this work, we have studied the dynamic structure of reversible β-casein micelles in the absence of calcium phosphate. We have discovered a new slow relaxation process, which seem a characteristic feature of unfolded proteins. One of the most surprising results of our study is the complete independence of the dynamic flexibility from the reversible association of micelles. This should contrast with folding/unfolding of a protein, in which the change of the atomic packing affects the internal structural dynamics (61–63).

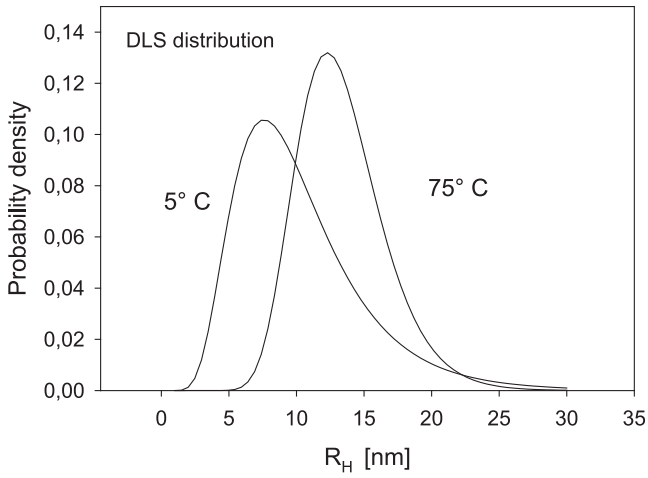

FIGURE 9 Log-normal distribution of the hydrodynamic radii of the β-casein for 82 mg/mL at two temperatures based on a DLS cumulant analysis (see section S1. Polydispersity and Cumulant Analysis in DLS in Supporting materials and methods).

CONCLUSIONS

In this study, effects of micellization of β-casein on the nanosecond structural dynamics were examined by quasielastic neutron scattering. The self-association little affects the internal dynamics of β-casein on a nanosecond timescale. In contrast, this type of internal structural dynamics is changed upon the folding and unfolding of a globular protein because of the change of the atomic packing. The dynamical change upon the folding or unfolding might also be related to the change of the hydration state because the protein folding is accompanied by dehydration of the polypeptide chain. The slower internal dynamics of β-casein in a nanosecond timescale seems to be a characteristic feature of the unfolded structure. It requires bulk solvent and is not seen in hydrated protein powder. This is compatible with the previous discussion that the casein micelle holds a relatively large amount of hydration water inside the micelle. In the next step, it would be interesting to study the effect of calcium binding on the internal structural dynamics to discuss the relationship among structure, dynamics, and biological function.

SUPPORTING MATERIAL

Supporting material can be found online at https://doi.org/10.1016/j.bpj.2021.10.032.

AUTHOR CONTRIBUTIONS

H.N., M.-S.A., and W.D. designed and carried out whole research. J.W. and M.Z. contributed to neutron backscattering experiments. O.H. contributed NSE experiments. T.E.S. contributed dynamic light scattering experiment. D.R. contributed neutron scattering data analysis. H.N., M.-S.A., and W.D. wrote the manuscript. All authors read and approved the final the manuscript. H.N., M.-S.A., and W.D. contributed equally.

ACKNOWLEDGMENTS

We thank Dr. Jörg Stellbrink (JCNS-1/IBI-8 Forschungszentrum Jülich) for his help with the DLS experiment and Prof. Marco Heinen (Universidad de Guanajuato/formerly ICS at Forschungszentrum Jülich) for providing his program for the RMSA model, which helped to complete the SANS and quasielastic neutron scattering analysis. The work is based upon experiments performed at the KWS-1, Jülich NSE, and SPHERES at the JCNS at MLZ in Garching, Germany.

This work was partly supported by JSPS KAKENHI grant numbers JP18H05229 and JP20H02944.

REFERENCES

1. Warshel, A., and R. P. Bora. 2016. Perspective: defining and quantifying the role of dynamics in enzyme catalysis. *J. Chem. Phys.* 144:180901.
2. Go, N. 1983. Theoretical studies of protein folding. *Annu. Rev. Biophys. Bioeng.* 12:183–210.
3. Bryngelson, J. D., and P. G. Wolynes. 1987. Spin glasses and the statistical mechanics of protein folding. *Proc. Natl. Acad. Sci. USA.* 84:7524–7528.
4. Go, N., T. Noguti, and T. Nishikawa. 1983. Dynamics of a small globular protein in terms of low-frequency vibrational modes. *Proc. Natl. Acad. Sci. USA.* 80:3696–3700.
5. Holt, C., N. M. Wahlgren, and T. Drakenberg. 1996. Ability of a beta-casein phosphopeptide to modulate the precipitation of calcium phosphate by forming amorphous dicalcium phosphate nanoclusters. *Biochem. J.* 314:1035–1039.
6. Smith, J. C., K. Kuczera, …, M. Karplus. 1989. Internal dynamics of globular proteins, comparison of neutron scattering measurements and theoretical models. *Physica B.* 156:437–443.
7. Smith, J., K. Kuczera, and M. Karplus. 1990. Dynamics of myoglobin: comparison of simulation results with neutron scattering spectra. *Proc. Natl. Acad. Sci. USA.* 87:1601–1605.
8. Loncharich, R. J., and B. R. Brooks. 1990. Temperature dependence of dynamics of hydrated myoglobin. Comparison of force field calculations with neutron scattering data. *J. Mol. Biol.* 215:439–455.
9. Doster, W., S. Cusack, and W. Petry. 1989. Dynamical transition of myoglobin revealed by inelastic neutron scattering. *Nature.* 337:754–756.
10. Cusack, S., and W. Doster. 1990. Temperature dependence of the low frequency dynamics of myoglobin. Measurement of the vibrational frequency distribution by inelastic neutron scattering. *Biophys. J.* 58:243–251.
11. Doster, W., A. Bachleitner, …, E. Lüscher. 1986. Thermal properties of water in myoglobin crystals and solutions at subzero temperatures. *Biophys. J.* 50:213–219.
12. Gaspar, A. M., S. Busch, …, W. Doster. 2010. Using polarization analysis to separate the coherent and incoherent scattering from protein samples. *Biochim. Biophys. Acta.* 1804:76–82.
13. Gaspar, A. M., M.-S. Appavou, …, W. Doster. 2008. Dynamics of well-folded and natively disordered proteins in solution: a time-of-flight neutron scattering study. *Eur. Biophys. J.* 37:573–582.
14. Farrell, H. M., E. L. Malin, …, P. X. Qi. 2006. Casein micelle structure: what can be learned from milk synthesis and structure biology? *Curr. Opin. Coll. Inter. Sci.* 11:135–147.
15. Garnier, J. 1966. Conformation de la caséine β en solution. Analyse d'une transition thermique entre 5 et 40°C. *J. Mol. Biol.* 19:586–590.
16. O'Connell, J. E., V. Y. Grinberg, and C. G. de Kruif. 2003. Association behavior of β-casein. *J. Colloid Interface Sci.* 258:33–39.
17. Faizullina, D. A., T. A. Konnovaa, …, Y. F. Zueva. 2013. Self-assembly and secondary structure of beta-casein. *Russ. J. Bioorganic Chem.* 39:366–372.
18. de Kruif, C. G., and V. Y. Grinberg. 2002. Micellisation of β-casein. *Colloids Surf. A Physicochem. Eng.* 210:183–190.
19. Kegeles, G. A. 1979. A Shell model for size distribution in micelles. *J. Phys. Chem.* 83:1728–1732.
20. Payens, T. A., and K. Heremans. 1969. Effect of pressure on the temperature-dependent association of β-casein. *Biopolymers.* 8:335–345.
21. Gebhardt, R., N. Takeda, …, W. Doster. 2011. Structure and stabilizing interactions of casein micelles probed by high-pressure light scattering and FTIR. *J. Phys. Chem. B.* 115:2349–2359.
22. Farrell, H. M., E. D. Wickham, …, P. D. Hoagland. 2001. Secondary structural studies of bovine caseins: a temperature dependence of β-casein structure as analysed by circular dichroism and FTIR spectroscopy and correlation with micellization. *Food Hydrocoll.* 15:341–354.
23. Leclerc, E., and P. Calmettes. 1997. Interactions in micellar solutions of β-casein. *Phys. Rev. Lett.* 78:150–153.
24. Doster, W., and M. Settles. 2005. Protein-water displacement distributions. *Biochim. Biophys. Acta.* 1749:173–186.
25. Doster, W., H. Nakagawa, and M.-S. Appavou. 2013. Scaling analysis of bio-molecular dynamics derived from elastic incoherent neutron scattering experiments. *J. Chem. Phys.* 139:045105.
26. Doster, W. 2019. Time domain versus energy domain neutron scattering analysis of protein dynamics. *Proc. Natl. Acad. Sci. USA.* 116:8649–8650.
27. Doster, W. 2018. Are proteins dynamically heterogeneous? Neutron scattering analysis of hydrogen displacement distributions. *Int. J. Mol. Theor. Phys.* 2:1–14.
28. Perticaroli, S., J. D. Nickels, …, A. P. Sokolov. 2014. Dynamics and rigidity in an intrinsically disordered protein, β-casein. *J. Phys. Chem. B.* 118:7317–7326.
29. Dhindsa, G. K., M. Tyagi, and X. Q. Chu. 2014. Temperature-dependent dynamics of dry and hydrated β-casein studied by quasielastic neutron scattering. *J. Phys. Chem. B.* 118:10821–10829.
30. Gallat, F. X., A. Laganowsky, …, M. Weik. 2012. Dynamical coupling of intrinsically disordered proteins and their hydration water: comparison with folded soluble and membrane proteins. *Biophys. J.* 103:129–136.
31. Stadler, A. M., L. Stingaciu, …, D. Richter. 2014. Internal nanosecond dynamics in the intrinsically disordered myelin basic protein. *J. Am. Chem. Soc.* 136:6987–6994.
32. Grimaldo, M., F. Roosen-Runge, …, T. Seydel. 2019. Dynamics of proteins in solution. *Q. Rev. Biophys.* 52:1–63.
33. Feoktystov, A., H. Frielinghaus, …, T. Brückel. 2015. KWS-1 high resolution SANS instrument at JCNS: current state. *J. Appl. Cryst.* 48:61–70.
34. Hayter, J. B., and J. Penfold. 1981. An analytic structure factor for macroion solutions. *Mol. Phys.* 42:109–118.
35. Hansen, J.-P., and J. B. Hayter. 1982. A rescaled MSA structure factor for dilute charged colloidal dispersions. *Mol. Phys.* 46:651–656.
36. Pipich, V.. QtiKWS: visualisation, reduction, analysis and fit framework with focus on Small Angle Scattering. http://qtisas.com/qtikws.
37. Bee, M. 1988. Quasi-Elastic Neutron Scattering. Adam Hilger, Bristol, UK, pp. 72–105.
38. Holderer, O., M. Monkenbusch, …, D. Richter. 2008. The JCNS neutron spin-echo spectrometer J-NSE at the FRM II. *Meas. Sci. Technol.* 19:034022.
39. Wuttke, J., A. Budwig, …, S. Staringer. 2012. SPHERES, Jülich's high-flux neutron backscattering spectrometer at FRM II. *Rev. Sci. Instrum.* 83:075109.
40. Fitter, J. 2003. Conformational dynamics of a protein in the folded and the unfolded state. *Chem. Phys.* 292:405–411.
41. Perticaroli, S., G. Ehlers, …, J. D. Nickels. 2017. Description of hydration water in protein (green fluorescent protein) solution. *J. Am. Chem. Soc.* 139:1098–1105.
42. Wuttke, J. (2006). FRIDA: fast reliable inelastic data analysis. https://jugit.fz-juelich.de/mlz/frida

43. Biehl, R., B. Hoffmann, …, D. Richter. 2008. Direct observation of correlated interdomain motion in alcohol dehydrogenase. *Phys. Rev. Lett.* 101:138102.

44. Andrews, A. L., D. Atkinson, …, R. N. Robertson. 1979. The conformation and aggregation of bovine β-casein A. I. Molecular aspects of thermal aggregation. *Biopolymers.* 18:1105–1121.

45. Hofmann, H., A. Soranno, …, B. Schuler. 2012. Polymer scaling laws of unfolded and intrinsically disordered proteins quantified with single-molecule spectroscopy. *Proc. Natl. Acad. Sci. USA.* 109:16155–16160.

46. Maxwell, J. C. 1867. IV. On the dynamical theory of gases. *Trans. Roy. Soc. (London).* 157:49–88.

47. Kleinert, T., W. Doster, …, M. Settles. 1998. Solvent composition and viscosity effects on the kinetics of CO binding to horse myoglobin. *Biochemistry.* 37:717–733.

48. Longeville, S., and W. Doster. 2012. Chapter 8. Protein dynamics and function. *In* Dynamics of Soft Matter, Neutron Applications. V. G. Sakai, C. Alba-Simionesco, and S.-H. Chen, eds. Springer Science and Business Media.

49. Volino, F., J. C. Perrin, and S. Lyonnard. 2006. Gaussian model for localized translational motion: application to incoherent neutron scattering. *J. Phys. Chem. B.* 110:11217–11223.

50. Fitter, J. 2003. A measure of conformational entropy change during thermal protein unfolding using neutron spectroscopy. *Biophys. J.* 84:3924–3930.

51. Risken, H. 1996. The Fokker Planck Equation, Methods of Solution and Application, part of the Springer Series in Synergetics. Springer-Verlag, Berlin, pp. 96–132.

52. Doster, W. 2006. Brownian oscillator analysis of molecular motions in biomolecules. *In* Neutron Scattering in Biology, Techniques and Applications, Biological and medical Physics. J. Fitter, T. Gutberlet, and J. Katsaras, eds. Springer, pp. 461–482.

53. Uhlenbeck, G. E., and L. S. Ornstein. 1930. On the theory of the brownian motion. *Phys. Rev.* 36:823–841.

54. Bicout, D. J., and G. Zaccai. 2001. Protein flexibility from the dynamical transition: a force constant analysis. *Biophys. J.* 80:1115–1123.

55. Marshall, B. T., K. K. Sarangapani, …, C. Zhu. 2006. Measuring molecular elasticity by atomic force microscope cantilever fluctuations. *Biophys. J.* 90:681–692.

56. Bu, Z., R. Biehl, …, D. J. E. Callaway. 2005. Coupled protein domain motion in Taq polymerase revealed by neutron spin-echo spectroscopy. *Proc. Natl. Acad. Sci. USA.* 102:17646–17651.

57. Pérez, J., J.-M. Zanotti, and D. Durand. 1999. Evolution of the internal dynamics of two globular proteins from dry powder to solution. *Biophys. J.* 77:454–469.

58. Stadler, A. M., F. Demmel, …, T. Seydel. 2016. Picosecond to nanosecond dynamics provide a source of conformational entropy for protein folding. *Phys. Chem. Chem. Phys.* 18:21527–21538.

59. Richter, D., B. Ewen, …, T. Wagner. 1989. Microscopic dynamics and topological constraints in polymer melts: a neutron-spin-echo study. *Phys. Rev. Lett.* 62:2140–2143.

60. Gebhardt, R., W. Doster, …, U. Kulozik. 2006. Size distribution of pressure-decomposed casein micelles studied by dynamic light scattering and AFM. *Eur. Biophys. J.* 35:503–509.

61. Bu, Z., D. A. Neumann, …, C. C. Han. 2000. A view of dynamics changes in the molten globule-native folding step by quasielastic neutron scattering. *J. Mol. Biol.* 301:525–536.

62. Grimaldo, M., F. Roosen-Runge, …, T. Seydel. 2015. Hierarchical molecular dynamics of bovine serum albumin in concentrated aqueous solution below and above thermal denaturation. *Phys. Chem. Chem. Phys.* 17:4645–4655.

63. Ameseder, F., A. Radulescu, …, A. M. Stadler. 2018. Homogeneous and heterogeneous dynamics in native and denatured bovine serum albumin. *Phys. Chem. Chem. Phys.* 20:5128–5139.